The Canadian Mineralogist
Vol. 54, pp. 145-162 (2016)
DOI: 10.3749/canmin.1500062

VANARSITE, PACKRATITE, MORRISONITE, AND GATEWAYITE: FOUR NEW MINERALS CONTAINING THE $[As^{3+}V^{4+,5+}_{12}As^{5+}_{6}O_{51}]$ HETEROPOLYANION, A NOVEL POLYOXOMETALATE CLUSTER

ANTHONY R. KAMPF[§]

Mineral Sciences Department, Natural History Museum of Los Angeles County, 900 Exposition Boulevard, Los Angeles, California 90007, U.S.A.

JOHN M. HUGHES

Department of Geology, University of Vermont, 180 Colchester Ave., Burlington, Vermont 05405, U.S.A.

BARBARA P. NASH

Department of Geology and Geophysics, University of Utah, Salt Lake City, Utah 84112, U.S.A.

JOE MARTY

5199 E. Silver Oak Rd., Salt Lake City, Utah 84108, U.S.A.

ABSTRACT

Vanarsite (IMA2014-031), $NaCa_{12}(As^{3+}V^{4+}_{3.5}V^{5+}_{8.5}As^{5+}_{6}O_{51})_2 \cdot 78H_2O$, packratite (IMA2014-059), $Ca_{11}(As^{3+}V^{4+}_{2}V^{5+}_{10}As^{5+}_{6}O_{51})_2 \cdot 83H_2O$, morrisonite (IMA2014-088), $Ca_{11}(As^{3+}V^{4+}_{2}V^{5+}_{10}As^{5+}_{6}O_{51})_2 \cdot 78H_2O$, and gatewayite (IMA2014-096), $Ca_6(As^{3+}V^{4+}_{3}V^{5+}_{9}As^{5+}_{6}O_{51}) \cdot 31H_2O$, are four new minerals from the Packrat mine, Gateway district, Mesa County, Colorado, U.S.A. Crystals of all four new minerals are very dark blue to greenish-blue blades. They are found together on montroseite- and corvusite-bearing sandstone in association with pharmacolite. Vanarsite is monoclinic, $P2_1/c$, a 25.8902(8), b 10.9468(3), c 28.2980(8) Å, β 102.252(1)°, V 7828.9(3) Å^3, and Z = 2. Packratite is triclinic, $P\overline{1}$, a 18.0572(4), b 19.4126(4), c 24.0586(17) Å, α 87.364(6), β 86.266(6), γ 79.267(6)°, V 8263.4(7) Å^3, and $Z = 2$. Morrisonite is monoclinic, $P2_1/c$, a 14.9566(18), b 48.208(6), c 23.836(3) Å, β 90.034(6)°, V 17187(4) Å^3, and Z = 4. Gatewayite is monoclinic, $P2_1$, a 11.1850(4), b 16.8528(4), c 20.7146(15) Å, β 91.166(6)°, V 3903.9(3) Å^3, and $Z = 2$. The structures of all four new minerals contain the novel polyoxometalate-like heteropolyanion, $[As^{3+}As^{5+}_{6}V^{4+}_{2+x}V^{5+}_{10-x}O_{51}]^{(11+x)-}$ ($x = 0$ to 1.5), which is new to science.

Keywords: Vanarsite, packratite, morrisonite, gatewayite, new mineral, crystal structure, polyoxometalate, Packrat mine, Gateway, Colorado.

INTRODUCTION

The field of polyoxometalate (POM) chemistry has been extremely active over the last few decades as POM clusters have proven to have a remarkable array of technological and biochemical uses (*cf.* Aureliano 2011, Cronin & Müller 2012, Song & Tsunashima 2012). Thousands of POM compounds are now known and hundreds of new ones are synthesized each year. However, there are very few known POM or POM-like minerals. Best known are the pascoite-family minerals, which contain the decavanadate cluster anion $[V_{10}O_{28}]^{6-}$, an isopolyanion, and its protonated and mixed-valence V^{4+}/V^{5+} variants. Over the last several years, our studies of the secondary mineralization in U–V deposits of western Colorado and eastern Utah have yielded many new members of the pascoite family (*cf.* Kampf *et al.* 2014a). One of these U–V deposits, the

[§] *Corresponding author e-mail address*: akampf@nhm.org

TABLE 1. FORMULAS, PHYSICAL AND OPTICAL PROPERTIES FOR VANARSITE FAMILY MINERALS

	vanarsite	packratite	morrisonite	gatewayite
IMA #	2014-031	2014-059	2014-088	2014-096
Ideal formula	$NaCa_{12}(As^{3+}V^{4+}{}_{3.5}V^{5+}{}_{8.5}As^{5+}{}_{6}O_{51})_2 \cdot 78H_2O$	$Ca_{11}(As^{3+}V^{4+}{}_{2}V^{5+}{}_{10}As^{5+}{}_{6}O_{51})_2 \cdot 83H_2O$	$Ca_{11}(As^{3+}V^{4+}{}_{2}V^{5+}{}_{10}As^{5+}{}_{6}O_{51})_2 \cdot 78H_2O$	$Ca_6(As^{3+}V^{4+}{}_{3}V^{5+}{}_{9}As^{5+}{}_{6}O_{51}) \cdot 31H_2O$
Color	very dark blue	very dark greenish blue	very dark blue	very dark greenish blue
Streak	grayish blue	grayish blue	grayish blue	grayish blue
Luster	vitreous	vitreous	vitreous	vitreous
Transparency	transparent	transparent	transparent	transparent
Fluorescence	none	none	none	none
Hardness (Mohs)	~2	~2	2½	~2
Fracture	curved	curved	curved	curved
Tenacity	brittle	brittle	brittle	brittle
Cleavage	{100} fair	{001}, {110}, and {1–10} fair	{010} perfect, {100} good	{010} and {101} fair
D_{meas} (g/cm^3)	2.48(2)	2.36(2)	2.29(2)	2.34(2)
D_{calc} (g/cm^3)	2.460	2.351	2.221	2.337
Chem. tests	insol. RT H_2O; easily sol. RT dil. HCl.	insol. RT H_2O; easily sol. RT dil. HCl.	insol. RT H_2O; easily sol. RT dil. HCl.	insol. RT H_2O; easily sol. RT dil. HCl.
Optical class	biaxial (–)	biaxial (–)	biaxial (–)	biaxial (–)
α	1.645(5)	1.625(calc)	1.611(2)	1.621(1)
β	1.677(calc)	1.628(2)	1.631(calc)	1.654(5)
γ	1.681(calc)	1.629(2)	1.637(2)	1.668(5)
$2V_{meas}$	37(2)°	60.7(4)°	58(1)°	65.9(9)°
$2V_{calc}$	–	–	–	65.0°
Dispersion	not observable	r < v, moderate	not observable	extreme
Orientation	$X = \mathbf{b}$, $Y \wedge \mathbf{a} = 12°$ in obtuse β	$X \approx \perp$ {110}, $Z \wedge \mathbf{c} \approx 20°$	$X \approx \mathbf{a}$, $Y = \mathbf{b}$, $Z \approx \mathbf{c}$	$Y = \mathbf{b}$, $X \wedge$ a $\approx 30°$ in obtuse β
Pleochroism	*X* cornflower blue, *Y* dark blue, *Z* dark blue; $X << Z \approx Y$	nonpleochroic dark blue	*X* blue, *Y* dark blue, *Z* dark blue; $X << Y \approx Z$	*X* pale olive green, *Y* medium greenish blue, *Z* dark greenish blue; $X << Y < Z$
Gladstone-Dale	–0.001	0.027	–0.028	–0.031
Compatibility	superior	excellent	excellent	excellent

Packrat mine in Colorado, has also yielded four new minerals containing the novel POM-like heteropolyanion, $[As^{3+}As^{5+}{}_{6}V^{4+}{}_{2+x}V^{5+}{}_{10-x}O_{51}]^{(11+x)-}$ ($0 \le x \le 1.5$), which is new to science.

Although the $[As^{3+}V^{4+,5+}{}_{12}As^{5+}{}_{6}O_{51}]$ heteropolyanion described herein was previously unknown, other arsenic and mixed-valence vanadium POMs have been synthesized. Wutkowski *et al*. (2011) describe the atomic arrangement of an arsenato-polyoxovanadate cluster compound with the composition $(NH_4)_4[V_8{}^{4+}V_4{}^{5+}As_8{}^{3+}O_{40}(H_2O)] \cdot 4H_2O$, with the cluster composition in brackets, and reference numerous other synthetic arsenic and mixed-valence vanadium POMs. However, we have been unable to find in the literature a synthetic POM with both mixed valence As and V, and the minerals described herein may be the first compounds with that type of polyoxometalate cluster. It is of interest that the V^{4+} and V^{5+} are mixed in VO_6 octahedra, whereas the As^{3+} and As^{5+} require their own unique polyhedra, $As^{5+}O_4$ tetrahedra and an $As^{3+}O_3\psi$ tetrahedron, where ψ represents the As^{3+} lone pair electrons.

These four new minerals, vanarsite, packratite, morrisonite, and gatewayite (Table 1), are described herein and should be referred to as the vanarsite mineral family because vanarsite was the first of them to be approved. The name vanarsite is based on the composition of the mineral and specifically the fact that it contains vanadate, arsenite, and arsenate groups. Packratite is named for the locality, the Packrat mine. Morrisonite is named for the Morrison Formation, in which the Packrat mine and other U–V mines of the Uravan mineral belt occur. As a point of further interest, the Jurassic Morrison Formation is more

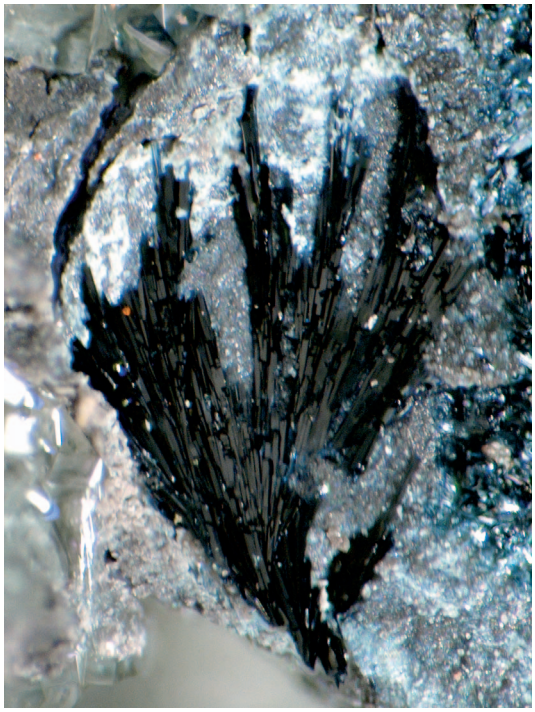

FIG. 1. Subparallel intergrowth of vanarsite blades forming finger-like aggregates; FOV 3 mm.

widely known as being the most prolific source of dinosaur fossils in North America. Gatewayite is named for the Gateway mining district in which the Packrat mine is located. Gateway is also the nearest town to the Packrat mine.

The new minerals and their names have been approved by the Commission on New Minerals, Nomenclature, and Classification of the International Mineralogical Association (Table 1). All type [holotype (HT) and cotype (CT)] specimens for the minerals are deposited in the collections of the Natural History Museum of Los Angeles County, Los Angeles, California, under the following catalogue numbers: 64149 (vanarsite CT and morrisonite CT), 64150 (vanarsite CT), 64513 (packratite HT and gatewayite CT), 64514 (packratite CT and gatewayite CT), 65554 (morrisonite CT and gatewayite CT), 65555 (morrisonite CT and gatewayite CT), 65556 (morrisonite CT), and 65559 (gatewayite CT).

OCCURRENCE

Vanarsite, packratite, morrisonite, and gatewayite were found in the main tunnel level of the Packrat mine, Gateway district, Mesa County, Colorado, USA (38°38′51.28″N 109°02′49.77″W). The Packrat mine is near the northern end of the Uravan Mineral Belt, in which uranium and vanadium minerals occur together in bedded or roll-front deposits in the sandstone of the Salt Wash member of the Jurassic Morrison Formation (Carter & Gualtieri 1965, Shawe 2011). The original Packrat #1 and #2 claims were filed in 1943, but mining apparently did not commence until the early 1950s. The mine remained in operation until 1990 and consists of several miles of drifts and numerous stopes. The mine site was reclaimed in 2002, and was reopened in 2007 for further exploration; it is currently inactive. The samples of the new minerals were collected on September 10, 2011, and May 3, 2013.

Vanarsite, packratite, morrisonite, and gatewayite are found together on montroseite- and corvusite-bearing sandstone. They are also closely associated with pharmacolite and a potentially new vanadate mineral, currently under study. Other secondary minerals found in the mine include andersonite, ansermetite, calcite, dickthomssenite, gypsum, hewettite, hummerite, lasalite, magnesiopascoite, martyite, munirite, navajoite, pascoite, picropharmacolite, postite, rossite, native selenium, sherwoodite, uranopilite, and at least two other potentially new minerals, currently under study.

The new minerals form from the oxidation of montroseite-corvusite assemblages in a moist environment. Mining operations have exposed unoxidized and oxidized phases. Under ambient temperatures and generally oxidizing near-surface conditions, water reacts with pyrite and an unknown As-bearing phase (perhaps arsenopyrite) to form aqueous solutions with relatively low pH. The various secondary vanadate phases that form depend upon prevailing Eh-pH conditions and the presence of other cations (*e.g.*, Na^{+}, Ca^{2+}, Mg^{2+}).

APPEARANCE, PHYSICAL PROPERTIES, AND OPTICAL PROPERTIES

Crystals of all four new minerals are very dark blue to greenish-blue blades. Vanarsite blades are flattened on {100} and elongated on [010]. They occur in sub-parallel intergrowths and form fan-like or finger-like aggregates up to about 5 mm in length (Fig. 1). Packratite blades are flattened on {110} and elongated on [001]. They are up to about 1 mm long, striated lengthwise, and grow in sub-parallel and divergent intergrowths (Fig. 2). The mineral also occurs as pearly green, botryoidal aggregates. Morrisonite blades are flattened on {010} and elongated on [100]. They are up to about 1 mm long, striated lengthwise, and grow in sub-parallel and divergent intergrowths (Fig. 3). Gatewayite blades are more or less flattened on {101} and elongated on [010]. They

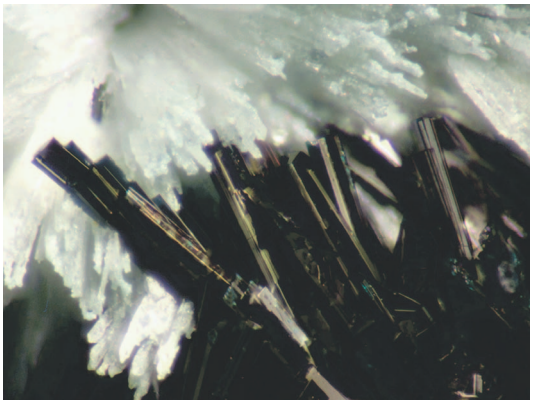

FIG. 2. Packratite needles with pharmacolite; FOV 1 mm.

are up to 0.5 mm long and form divergent intergrowths. Gatewayite also occurs as crude prisms, up to 1 mm long, with rounded faces (Fig. 4) and as composite crystals consisting of subparallel intergrowths of narrow prisms up to 2 mm long (Fig. 5). Crystal drawings of all four minerals are provided in Figures 6 through 9.

The chemical formulae and physical and optical properties of all four minerals are listed in Table 1. The densities were measured by floatation in mixtures of methylene iodide and toluene. The dark color made the optical determinations challenging and prevented conoscopic observations. The $2V$ for each mineral was measured using extinction data and the EXCALIBR program (Gunter *et al*. 2004). For vanarsite, the very dark color in the Y and Z optical directions prevented the measurement of β and γ; consequently, they were calculated based upon the retardation ($\alpha - \gamma = 0.04$), measured using a Berek compensator, and the $2V$ value. For packratite, it was impossible to measure α; consequently, it was calculated based upon β, γ, and $2V$. For morrisonite, it was impossible to measure β; consequently, it was calculated based upon α, γ, and $2V$. The dispersion for gatewayite is apparently extreme based upon extinction colors; however, the sense could not be determined.

FIG. 3. Morrisonite blades; FOV 1.3 mm.

FIG. 4. Crude prisms of gatewayite with curved faces; FOV 1 mm across.

CHEMICAL ANALYSIS

Analyses of all four phases were performed at the University of Utah using a Cameca SX-50 electron microprobe with four wavelength dispersive-spectrometers and employing Probe for EPMA software. Analytical conditions were 15 keV accelerating voltage, 10 nA beam current, and a beam diameter of 10–15 μm. Counting times were 10 s for each element except Na, which was analyzed with five-second count times. In the analytical routine, Na, Ca, As, and V were counted simultaneously, *i.e.*, first on their respective spectrometers. Standards were: albite (Na), diopside (Ca), Sr-titanate (Sr), GaAs (As), and YVO_4 (V). Raw X-ray intensities were corrected for matrix effects with a $\phi(\rho z)$ algorithm (Pouchou & Pichoir 1991).

There was moderate damage from the electron beam, but this did not seem to affect the relative

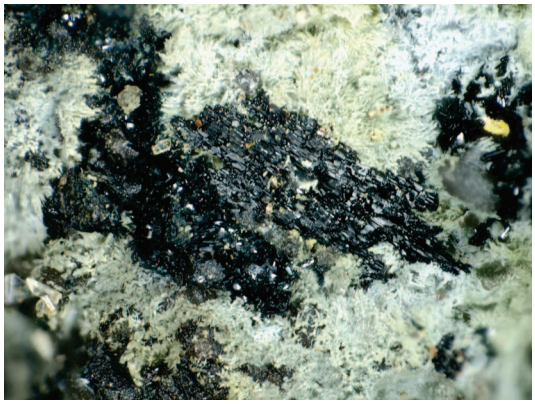

FIG. 5. Composite gatewayite crystal consisting of subparallel intergrowth of narrow prisms, associated with grey-white pharmacolite; 3 mm FOV across.

proportions of cations. However, as is typical of highly hydrated phases with weakly held H_2O, these phases partially dehydrate under vacuum in the microprobe chamber. The H_2O loss results in higher concentrations for the remaining constituents than is to be expected for the fully hydrated phases. Because insufficient material is available for a direct determination of H_2O, it was calculated based upon the structure determinations. The analyzed constituents

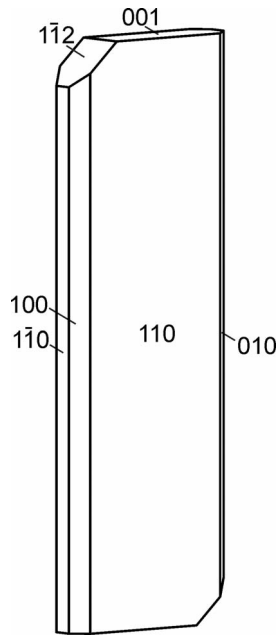

FIG. 7. Crystal drawing of packratite; clinographic projection in standard orientation.

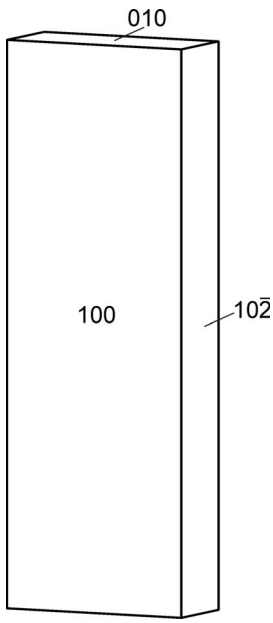

FIG. 6. Crystal drawing of vanarsite; clinographic projection in nonstandard orientation, *b* vertical.

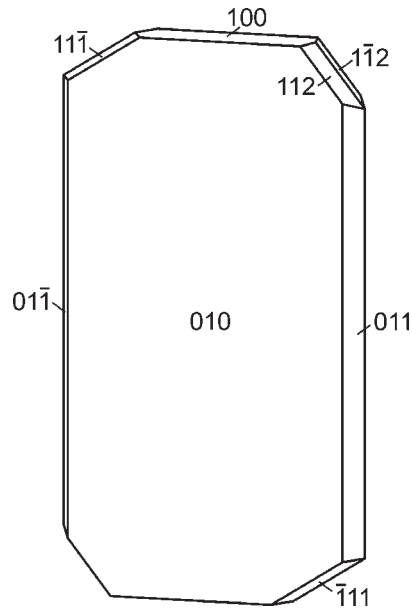

FIG. 8. Crystal drawing of morrisonite; clinographic projection in nonstandard orientation (**a** vertical).

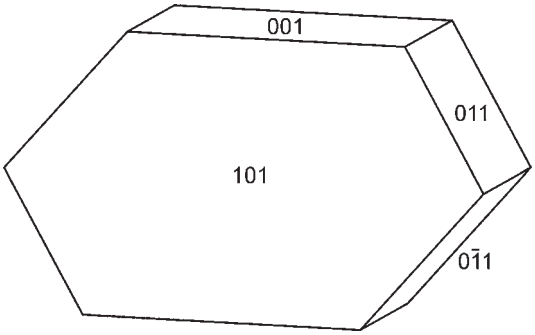

FIG. 9. Crystal drawing of gatewayite blade; clinographic projection in standard orientation.

were normalized to provide a total of 100% when combined with the calculated H_2O. Analytical data are given in Table 2.

X-ray Crystallography and Structure Determinations

Both powder and single-crystal X-ray studies were carried out using a Rigaku R-Axis Rapid II curved imaging plate microdiffractometer, with monochromatized Mo$K\alpha$ radiation (50 kV, 40 mA). For the powder-diffraction studies, a Gandolfi-like motion on the φ and ω axes was used to randomize the samples and observed *d*-values and intensities were derived by profile fitting using JADE 2010 software (Materials Data, Inc.). The strongest eight peaks in each powder

TABLE 2. ANALYTICAL DATA FOR VANARSITE FAMILY MINERALS

	vanarsite (16 points on 8 crystals)				packratite (4 points on 2 crystals)			
Const.	wt.%	Range	s.d.	Norm. wt.%	wt.%	Range	s.d.	Norm. wt.%
Na_2O	0.63	0.43–1.22	0.20	0.54	0.30	0.25–0.38	0.06	0.27
CaO	13.08	12.65–13.46	0.22	11.30	11.29	10.69–11.79	0.47	10.27
SrO	0.22	0.10–0.35	0.07	0.19				
FeO	0.04	0.00–0.08	0.03	0.03				
As_2O_3				3.41[a]				3.38[a]
As_2O_5	31.61	28.55–34.24	1.43	23.34[a]	31.28	29.33–34.22	2.08	24.49[a]
VO_2				9.55[a]				5.57[a]
V_2O_5	43.89	41.41–45.33	0.98	27.44[a]	40.23	38.53–41.76	1.53	30.46[a]
H_2O				24.20[b]				25.56[b]
Total	89.47			100.00	83.22			100.00
Empirical formula	$(Na_{1.01}Ca_{11.70}Sr_{0.11}Fe^{2+}_{0.02})_{\Sigma 12.84}$ $(As^{3+}_{1.00}V^{4+}_{3.34}V^{5+}_{8.76}As^{5+}_{5.90}O_{51})_2 \cdot 78H_2O$ based on: V + As = 38 and O = 180 *apfu*				$(Na_{0.51}Ca_{10.72})_{\Sigma 11.23}$ $(As^{3+}_{1.00}V^{4+}_{1.97}V^{5+}_{9.80}As^{5+}_{6.23}O_{51})_2 \cdot 83H_2O$ based on: V + As = 38 and O = 185 *apfu*			

	morrisonite (33 points on 13 crystals)				gatewayite (9 points on 7 crystals)			
Const.	wt.%	Range	s.d.	Norm. wt.%	wt.%	Range	s.d.	Norm. wt.%
Na_2O	0.21	0.01–0.57	0.13	0.18	0.21	0.09–0.37	0.10	0.19
CaO	11.82	10.98–12.30	0.39	10.35	12.31	11.90–12.79	0.32	11.31
SrO					0.41	0.20–0.66	0.18	0.38
FeO								
As_2O_3				3.44[a]				3.60[a]
As_2O_5	32.71	30.59–34.58	1.16	24.63[a]	32.18	29.62–34.43	1.58	25.40[a]
VO_2				5.14[a]				7.40[a]
V_2O_5	42.79	41.43–44.73	0.85	31.82[a]	42.97	41.95–44.32	0.76	31.39[a]
H_2O				24.44[b]				20.33[b]
Total	87.53			100.00	88.08			100.00
Empirical formula	$(Ca_{10.61}Na_{0.34})_{\Sigma 10.95}$ $(As^{3+}_{1.00}V^{4+}_{1.78}V^{5+}_{10.06}As^{5+}_{6.16}O_{51})_2 \cdot 78H_2O$ based on: V + As = 38 and O = 180 *apfu*				$(Ca_{5.54}Na_{0.17}Sr_{0.10})_{\Sigma 5.81}$ $(As^{3+}_{1.00}V^{4+}_{2.45}V^{5+}_{9.48}As^{5+}_{6.07}O_{51}) \cdot 31H_2O$ based on: V + As = 19 and O = 82 *apfu*			

[a] Total As was apportioned between As_2O_3 and As_2O_5 and total V was apportioned between VO_2 and V_2O_5, in both cases taking into account structural data and charge balance; excess or deficient As was placed in the As^{5+} sites. V^{4+}/V^{5+} assigned to balance charge of interstitial cations. [b] Based upon the crystal structure.

TABLE 3. STRONGEST POWDER X-RAY DIFFRACTION LINES FOR VANARSITE FAMILY MINERALS

Vanarsite		Packratite		Morrisonite		Gatewayite	
I_{obs}	d_{obs}(Å)	I_{obs}	d_{obs}(Å)	I_{obs}	d_{obs}(Å)	I_{obs}	d_{obs}(Å)
100	13.1	49	14.5	69	12.2	47	13.2
98	10.0	49	12.1	100	11.4	8	11.1
63	9.3	100	10.5	16	9.9	100	9.7
56	7.87	20	7.45	23	9.2	9	3.246
35	4.67	16	6.61	12	6.81	9	2.953
31	4.44	22	2.939	11	6.10	14	2.866
33	3.339	19	2.846	16	2.936	17	2.810
32	2.962	22	2.732	12	2.839	9	2.758

data set are listed in Table 3. The complete powder data have been deposited.

The Rigaku CrystalClear software package was used for processing the structure data, including the application of an empirical multi-scan absorption corrections using ABSCOR (Higashi 2001). The structures were solved by direct methods using SIR2004 (Burla *et al*. 2005). SHELXL-2013 software (Sheldrick 2008) was used for the full-matrix least-squares refinements on F^2. Because of their high H_2O contents, these minerals do not diffract strongly. The limited data sets for packratite, morrisonite, and

TABLE 4. DATA COLLECTION AND STRUCTURE REFINEMENT DETAILS FOR VANARSITE FAMILY MINERALS

	vanarsite	packratite	morrisonite	gatewayite
Crystal system	monoclinic	triclinic	monoclinic	monoclinic
Space group	$P2_1/c$	$P\bar{1}$	$P2_1/c$	$P2_1$
a (Å)	25.8815(5)	18.0572(4)	14.9566(18)	11.1850(4)
b (Å)	10.9416(2)	19.4126(4)	48.208(6)	16.8528(4)
c (Å)	28.2861(6)	24.0586(17)	23.838(3)	20.7146(15)
α (°)	–	87.364(6)	–	–
β (°)	102.2150(10)	86.266(6)	90.034(6)	91.166(6)
γ (°)	–	79.267(6)	–	–
Volume (Å^3)	7828.9(3)	8263.4(7)	17187(4)	3903.9(3)
Z	2	2	4	2
Abs. coeff.	4.839 mm^{-1}	4.555 mm^{-1}	4.345 mm^{-1}	4.835 mm^{-1}
F(000)	5706	5760	10680	2690
Crystal size	160 × 110 × 55 μm	110 × 50 × 10 μm	110 × 30 × 10 μm	150 × 70 × 40 μm
θ range	2.37 to 27.50°	3.00 to 21.49°	3.00 to 14.97°	3.03 to 25.03°
Index ranges	$-33 \le h \le 33$	$-18 \le h \le 18$	$-9 \le h \le 10$	$-13 \le h \le 12$
	$-14 \le k \le 12$	$-20 \le k \le 20$	$-31 \le k \le 34$	$-18 \le k \le 20$
	$-36 \le l \le 36$	$-24 \le l \le 23$	$-17 \le l \le 17$	$-24 \le l \le 21$
Reflections coll./unique	71450/17940	77672/18859	16415/6243	26034/12556
	$R_{int} = 0.063$	$R_{int} = 0.075$	$R_{int} = 0.103$	$R_{int} = 0.038$
$F > 4\sigma F$ refl.	14592	14753	4194	9088
Completeness	99.7%	99.5%	90.3%	97.5%
Parameters ref.	1289	2226	1233	842
GoF	1.062	1.031	1.035	1.096
Final R indices [$F_o > 4\sigma(F)$]	$R_1 = 0.0479$	$R_1 = 0.0395$	$R_1 = 0.0748$	$R_1 = 0.0533$
	$wR_2 = 0.1087$	$wR_2 = 0.0893$	$wR_2 = 0.1813$	$wR_2 = 0.1315$
R indices (all data)	$R_1 = 0.0633$	$R_1 = 0.0563$	$R_1 = 0.1178$	$R_1 = 0.0845$
	$wR_2 = 0.1193$	$wR_2 = 0.0968$	$wR_2 = 0.2168$	$wR_2 = 0.1602$
Ext. coeff.	Not refined	Not refined	0.0004(1)	Not refined
Abs. str. par.	dna	dna	dna	0.52(3)
Diff. peak/hole	+0.91/–1.23 e Å^{-3}	+0.98/–0.58 e Å^{-3}	+0.84/–0.70 e Å^{-3}	+2.12/–0.89 e Å^{-3}

TABLE 5. ATOM COORDINATES AND EQUIVALENT ISOTROPIC DISPLACEMENT PARAMETERS (Å^2) FOR VANARSITE

	x/*a*	*y*/*b*	*z*/*c*	U_{eq}		*x*/*a*	*y*/*b*	*z*/*c*	U_{eq}
Na	½	½	0	0.045(2)	H7B	0.509(2)	–0.183(5)	0.350(2)	0.048
Ca1	–0.07800(4)	–0.29986(11)	0.03462(4)	0.0278(2)	OW8	0.54324(19)	–0.1444(5)	0.26498(18)	0.0481(12)
Ca2	0.50479(4)	0.03079(10)	0.29507(4)	0.0263(2)	H8A	0.548(3)	–0.191(6)	0.2903(19)	0.058
Ca3	0.27953(4)	–0.44493(10)	–0.04994(4)	0.0272(2)	H8B	0.5727(18)	–0.140(7)	0.254(2)	0.058
Ca4	0.61167(4)	0.08547(11)	0.13529(4)	0.0295(2)	OW9	0.5889(2)	0.0247(5)	0.3519(3)	0.086(2)
Ca5	0.20887(4)	0.54636(10)	0.16984(4)	0.0273(2)	H9A	0.609(3)	0.093(5)	0.359(3)	0.103
Ca6	0.04444(6)	–0.20199(16)	0.24371(5)	0.0505(4)	H9B	0.608(3)	–0.033(6)	0.371(3)	0.103
As1	0.24671(2)	0.06349(5)	0.11144(2)	0.01919(11)	OW10	–0.1271(2)	–0.4409(4)	–0.02109(17)	0.0478(12)
As2	0.36854(2)	0.14893(5)	0.30507(2)	0.02147(11)	H10A	–0.124(3)	–0.520(3)	–0.015(2)	0.057
As3	0.14530(2)	0.05137(5)	0.27593(2)	0.02125(11)	H10B	–0.153(2)	–0.430(6)	–0.0461(19)	0.057
As4	0.04265(2)	–0.15646(5)	0.10641(2)	0.02011(11)	OW11	0.61929(17)	0.2823(4)	0.17415(16)	0.0412(10)
As5	0.15499(2)	–0.26870(5)	–0.04070(2)	0.02169(11)	H11A	0.5882(13)	0.310(6)	0.175(2)	0.049
As6	0.36330(2)	–0.15633(5)	–0.01847(2)	0.02187(11)	H11B	0.6422(18)	0.309(6)	0.1991(18)	0.049
As7	0.47412(2)	0.05529(5)	0.15999(2)	0.02246(11)	OW12	0.2776(3)	–0.6317(6)	–0.0969(2)	0.077(2)
V1	0.29877(3)	0.25339(8)	0.20455(3)	0.02048(17)	H12A	0.304(3)	–0.679(8)	–0.085(3)	0.092
V2	0.17939(3)	0.20048(8)	0.18912(3)	0.02059(17)	H12B	0.278(3)	–0.615(9)	–0.1272(15)	0.092
V3	0.11269(3)	0.07045(8)	0.07991(3)	0.02079(17)	OW13	0.03361(18)	–0.1302(5)	–0.0406(2)	0.0568(14)
V4	0.17149(3)	0.00947(8)	–0.00005(3)	0.02050(17)	H13A	0.022(3)	–0.101(8)	–0.0151(16)	0.068
V5	0.30624(3)	0.08027(8)	0.01572(3)	0.02086(17)	H13B	0.008(2)	–0.106(7)	–0.0662(16)	0.068
V6	0.36555(3)	0.19417(8)	0.11163(3)	0.02178(18)	OW14	0.21783(19)	0.4209(5)	0.09938(16)	0.0445(11)
V7	0.26301(3)	0.00120(8)	0.25899(3)	0.02007(17)	H14A	0.224(3)	0.341(3)	0.103(3)	0.053
V8	0.14749(3)	–0.22348(8)	0.06818(3)	0.01950(17)	H14B	0.243(2)	0.451(5)	0.086(3)	0.053
V9	0.38401(3)	–0.10835(8)	0.09505(3)	0.02030(17)	OW15	0.6499(2)	0.0176(5)	0.21503(17)	0.0475(12)
V10	0.37555(3)	–0.00472(8)	0.20935(3)	0.01975(17)	H15A	0.651(3)	–0.061(3)	0.221(2)	0.057
V11	0.15093(3)	–0.11222(8)	0.18306(3)	0.01950(17)	H15B	0.652(3)	0.058(5)	0.2415(17)	0.057
V12	0.26616(3)	–0.22014(8)	0.03247(3)	0.01972(17)	OW16	0.3415(2)	–0.4185(5)	–0.09872(18)	0.0550(13)
O1	0.28996(13)	0.1434(3)	0.07920(12)	0.0214(7)	H16A	0.332(3)	–0.439(7)	–0.1297(13)	0.066
O2	0.18585(12)	0.0895(3)	0.06689(12)	0.0212(7)	H16B	0.366(2)	–0.362(6)	–0.097(2)	0.066
O3	0.23845(13)	0.1920(3)	0.15039(12)	0.0215(7)	OW17	–0.00059(16)	–0.3575(5)	0.00424(17)	0.0437(11)
O4	0.40208(14)	0.2039(4)	0.35741(13)	0.0300(8)	H17A	0.0296(18)	–0.349(7)	0.0264(17)	0.052
O5	0.31597(13)	0.0689(4)	0.31518(12)	0.0247(8)	H17B	0.006(3)	–0.323(7)	–0.0222(15)	0.052
O6	0.40781(13)	0.0606(4)	0.27825(12)	0.0258(8)	OW18	0.2856(2)	0.6761(5)	0.1790(2)	0.0669(16)
O7	0.34883(14)	0.2683(4)	0.26712(13)	0.0285(8)	H18A	0.297(3)	0.752(3)	0.181(3)	0.080
O8	0.11118(15)	0.0727(4)	0.31866(13)	0.0305(9)	H18B	0.296(4)	0.642(7)	0.2076(18)	0.080
O9	0.20989(13)	0.0259(4)	0.30053(12)	0.0248(8)	OW19	0.0406(3)	0.3511(6)	0.1203(3)	0.0753(18)
O10	0.11943(14)	–0.0688(4)	0.24087(13)	0.0275(8)	H19A	0.044(4)	0.350(8)	0.1524(12)	0.090
O11	0.13824(14)	0.1768(4)	0.23940(13)	0.0274(8)	H19B	0.055(4)	0.284(5)	0.112(3)	0.090

TABLE 5. (CONTINUED)

	x/*a*	*y*/*b*	*z*/*c*	U_{eq}		*x*/*a*	*y*/*b*	*z*/*c*	U_{eq}
O12	–0.02105(13)	–0.1937(4)	0.09680(13)	0.0264(8)	OW20	0.4512(2)	0.1583(6)	0.0106(2)	0.0649(16)
O13	0.07183(13)	–0.1643(4)	0.16569(12)	0.0261(8)	H20A	0.425(2)	0.138(7)	0.025(3)	0.078
O14	0.07301(13)	–0.2579(3)	0.07610(12)	0.0236(7)	H20B	0.440(3)	0.222(6)	–0.008(3)	0.078
O15	0.04702(13)	–0.0103(3)	0.08772(13)	0.0258(8)	OW21	0.0748(2)	–0.4035(6)	0.2290(2)	0.0656(15)
O16	0.12740(16)	–0.3437(4)	–0.09074(13)	0.0321(9)	H21A	0.097(3)	–0.351(5)	0.249(3)	0.079
O17	0.12402(13)	–0.3061(4)	0.00453(13)	0.0255(8)	H21B	0.084(3)	–0.475(4)	0.245(3)	0.079
O18	0.21968(13)	–0.3087(4)	–0.02365(13)	0.0267(8)	OW22	0.2494(2)	0.3569(5)	0.31685(18)	0.0519(13)
O19	0.15270(14)	–0.1152(4)	–0.05165(13)	0.0260(8)	H22A	0.234(3)	0.353(7)	0.3417(18)	0.062
O20	0.39119(15)	–0.1985(4)	–0.06376(13)	0.0308(8)	H22B	0.236(3)	0.299(6)	0.296(2)	0.062
O21	0.40792(13)	–0.1579(4)	0.03457(12)	0.0254(8)	OW23	–0.0349(2)	–0.2514(6)	0.18818(17)	0.0554(14)
O22	0.31318(14)	–0.2541(4)	–0.01588(13)	0.0275(8)	H23A	–0.032(3)	–0.240(7)	0.1573(14)	0.066
O23	0.33761(14)	–0.0138(3)	–0.03040(13)	0.0270(8)	H23B	–0.061(2)	–0.307(6)	0.185(2)	0.066
O24	0.53830(14)	0.0824(4)	0.17110(13)	0.0320(9)	OW24	–0.1386(2)	–0.3366(5)	0.08700(18)	0.0540(13)
O25	0.45979(13)	–0.0619(3)	0.12024(13)	0.0256(8)	H24A	–0.161(3)	–0.277(5)	0.092(2)	0.065
O26	0.44220(13)	0.1852(4)	0.13704(13)	0.0262(8)	H24B	–0.128(3)	–0.371(6)	0.1165(16)	0.065
O27	0.45468(13)	0.0223(4)	0.21248(13)	0.0275(8)	OW25	0.5392(2)	–0.0131(6)	0.0710(2)	0.0623(16)
O28	0.13029(13)	0.1403(3)	0.13858(13)	0.0260(8)	H25A	0.510(2)	–0.036(7)	0.080(3)	0.075
O29	0.23890(13)	0.0350(4)	–0.00714(12)	0.0257(8)	H25B	0.539(3)	–0.057(7)	0.044(2)	0.075
O30	0.34839(14)	0.2345(4)	0.16820(13)	0.0291(8)	OW26	0.1239(3)	–0.5898(7)	0.2868(3)	0.092(2)
O31	0.28306(14)	0.3961(3)	0.19751(13)	0.0267(8)	H26A	0.145(4)	–0.655(7)	0.283(3)	0.110
O32	0.17074(14)	0.3462(3)	0.18407(13)	0.0262(8)	H26B	0.129(4)	–0.581(10)	0.3199(13)	0.110
O33	0.08496(13)	0.1808(3)	0.04578(13)	0.0264(8)	OW27	0.2222(3)	0.5599(6)	0.25482(19)	0.079(2)
O34	0.13921(14)	0.1226(4)	–0.02928(13)	0.0291(8)	H27A	0.222(4)	0.505(7)	0.278(3)	0.095
O35	0.30832(15)	0.2097(4)	–0.01073(14)	0.0316(9)	H27B	0.252(3)	0.603(8)	0.264(3)	0.095
O36	0.36572(16)	0.3256(4)	0.08605(13)	0.0315(9)	OW28	0.0768(4)	–0.0085(8)	–0.1299(2)	0.115(3)
O37	0.24465(13)	0.2014(3)	0.24216(12)	0.0208(7)	H28A	0.066(5)	0.061(6)	–0.117(4)	0.137
O38	0.11303(13)	–0.0581(3)	0.02857(12)	0.0216(7)	H28B	0.079(5)	–0.063(8)	–0.105(3)	0.137
O39	0.37746(13)	0.0802(3)	0.06005(12)	0.0225(7)	OW29	0.7073(2)	0.1494(7)	0.1434(3)	0.082(2)
O40	0.31357(12)	0.0518(3)	0.21794(12)	0.0213(7)	H29A	0.720(4)	0.085(6)	0.129(3)	0.098
O41	0.20028(13)	–0.0005(3)	0.20376(12)	0.0207(7)	H29B	0.711(4)	0.129(9)	0.1742(13)	0.098
O42	0.14810(12)	–0.0985(3)	0.11993(12)	0.0206(7)	OW30	0.5742(2)	–0.3708(7)	0.0458(2)	0.0705(17)
O43	0.20686(12)	–0.1518(3)	0.04377(12)	0.0200(7)	H30A	0.6088(15)	–0.382(9)	0.046(3)	0.085
O44	0.31142(13)	–0.1009(3)	0.05556(12)	0.0214(7)	H30B	0.576(3)	–0.354(9)	0.0783(14)	0.085
O45	0.36691(12)	0.0033(3)	0.14519(12)	0.0214(7)	OW31	0.4983(2)	0.2067(7)	0.3419(3)	0.095(3)
O46	0.27625(14)	–0.1419(4)	0.26520(14)	0.0300(8)	H31A	0.470(2)	0.221(9)	0.352(4)	0.115
O47	0.17765(14)	–0.2425(3)	0.19766(13)	0.0276(8)	H31B	0.520(3)	0.269(6)	0.346(4)	0.115
O48	0.17899(14)	–0.3319(3)	0.10057(12)	0.0250(8)	OW32	0.5215(2)	0.3437(8)	0.0565(2)	0.081(2)

TABLE 5. (CONTINUED)

	x/*a*	*y*/*b*	*z*/*c*	U_{eq}		*x*/*a*	*y*/*b*	*z*/*c*	U_{eq}
O49	0.28050(14)	–0.3309(4)	0.06917(14)	0.0282(8)	H32A	0.539(3)	0.421(4)	0.061(4)	0.097
O50	0.38249(14)	–0.2368(4)	0.12207(14)	0.0295(8)	H32B	0.550(3)	0.298(7)	0.051(4)	0.097
O51	0.37401(14)	–0.1469(4)	0.22102(13)	0.0278(8)	OW33	0.5514(3)	0.1735(7)	0.2589(2)	0.092(3)
OW1	0.4465(2)	–0.3966(5)	0.0473(2)	0.0580(14)	H33A	0.577(3)	0.121(9)	0.271(3)	0.111
H1A	0.441(3)	–0.316(3)	0.044(2)	0.070	H33B	0.546(4)	0.159(9)	0.2267(12)	0.111
H1B	0.453(3)	–0.411(6)	0.0790(12)	0.070	OW34	0.2210(2)	–0.3811(7)	–0.12188(19)	0.075(2)
OW2	0.6515(2)	–0.1027(4)	0.11634(16)	0.0435(11)	H34A	0.208(4)	–0.453(6)	–0.109(3)	0.090
H2A	0.652(3)	–0.100(6)	0.0852(12)	0.052	H34B	0.222(4)	–0.415(7)	–0.1515(17)	0.090
H2B	0.636(3)	–0.175(4)	0.120(2)	0.052	OW35	–0.0181(6)	–0.3010(14)	0.2925(4)	0.195(7)
OW3	0.23856(19)	–0.5907(4)	–0.0041(2)	0.0484(12)	H35A	–0.028(7)	–0.304(16)	0.321(3)	0.234
H3A	0.2063(13)	–0.602(6)	–0.018(3)	0.058	H35B	–0.014(9)	–0.379(6)	0.285(6)	0.234
H3B	0.256(2)	–0.660(4)	–0.005(3)	0.058	OW36	0.1035(4)	–0.2588(7)	0.3196(2)	0.071(3)
OW4	0.10974(17)	0.5475(4)	0.14706(18)	0.0425(11)	H36A	0.095(4)	–0.326(4)	0.334(3)	0.085
H4A	0.091(2)	0.480(4)	0.137(2)	0.051	H36B	0.091(4)	–0.196(5)	0.334(3)	0.085
H4B	0.095(2)	0.605(4)	0.126(2)	0.051	OW37	0.0200(3)	–0.0549(7)	0.2950(4)	0.075(4)
OW5	–0.05155(19)	–0.4918(5)	0.0767(2)	0.0557(14)	H37A	0.044(3)	–0.015(8)	0.317(3)	0.090
H5A	–0.027(2)	–0.528(6)	0.064(3)	0.067	H37B	0.000(3)	–0.016(11)	0.278(3)	0.090
H5B	–0.069(3)	–0.547(5)	0.089(3)	0.067	OW38*	–0.2060(5)	–0.1521(15)	0.1043(4)	0.201(10)
OW6	0.35396(19)	–0.5223(5)	0.00620(16)	0.0450(11)	OW39*	0.8020(10)	0.064(2)	0.1323(9)	0.31(2)
H6A	0.381(2)	–0.472(5)	0.019(2)	0.054	OW40*	0.0045(6)	–0.4970(14)	0.2914(6)	0.090(7)
H6B	0.353(3)	–0.576(5)	0.0304(19)	0.054	OW41*	0.7969(12)	0.224(3)	0.1847(11)	0.115(14)
OW7	0.48703(17)	–0.1211(4)	0.34976(17)	0.0399(10)	OW42*	0.0640(11)	–0.141(3)	0.3204(10)	0.029(10)
H7A	0.479(3)	–0.118(6)	0.3785(14)	0.048					

* Occ: OW38 = 0.87(2), OW39 = 0.70(3), OW40 = 0.46(2), OW41 = 0.29(2), OW42 = 0.13(2)

TABLE 6. SELECTED BOND DISTANCES (Å) IN VANARSITE

Ca1–O12	2.349(4)	Na–OW32	2.326(7)	V1–O31	1.615(4)	V7–O46	1.604(4)
Ca1–OW10	2.373(4)	Na–OW32	2.326(7)	V1–O30	1.819(4)	V7–O41	2.001(3)
Ca1–OW24	2.409(5)	Na–OW1	2.403(5)	V1–O7	1.967(4)	V7–O40	2.002(3)
Ca1–OW17	2.424(5)	Na–OW1	2.403(5)	V1–O37	2.012(3)	V7–O9	2.007(3)
Ca1–OW5	2.440(5)	Na–OW30	2.513(6)	V1–O3	2.055(3)	V7–O5	2.008(3)
Ca1–O34	2.489(4)	Na–OW30	2.513(6)	V1–O40	2.257(4)	V7–O37	2.271(4)
Ca1–O33	2.594(4)	<Na–O>	2.414	<V1–O>	1.954	<V7–O>	1.982
<Ca1–O>	2.44						
		As1–O1	1.811(3)				
Ca2–OW33	2.337(6)	As1–O2	1.819(3)	V2–O32	1.612(4)	V8–O48	1.611(4)
Ca2–OW31	2.362(5)	As1–O3	1.827(3)	V2–O28	1.823(4)	V8–O43	1.975(3)
Ca2–OW7	2.380(4)	<As1–O>	1.819	V2–O11	1.966(4)	V8–O17	1.991(4)
Ca2–OW8	2.397(5)			V2–O37	2.008(3)	V8–O42	2.001(3)
Ca2–OW9	2.418(5)	As2–O4	1.662(3)	V2–O3	2.063(3)	V8–O14	2.022(3)
Ca2–O27	2.422(4)	As2–O5	1.693(3)	V2–O41	2.281(4)	V8–O38	2.214(4)
Ca2–O6	2.475(3)	As2–O6	1.694(4)	<V2–O>	1.959	<V8–O>	1.969
<Ca2–O>	2.399	As2–O7	1.699(4)				
		<As2–O>	1.687				
Ca3–OW16	2.344(5)			V3–O33	1.616(4)	V9–O50	1.605(4)
Ca3–OW34	2.371(6)	As3–O8	1.657(4)	V3–O28	1.796(4)	V9–O44	1.974(3)
Ca3–OW6	2.378(4)	As3–O9	1.692(3)	V3–O15	1.969(3)	V9–O45	1.991(3)
Ca3–O18	2.379(4)	As3–O10	1.697(4)	V3–O2	2.015(3)	V9–O25	2.005(3)
Ca3–O22	2.386(4)	As3–O11	1.704(4)	V3–O38	2.023(4)	V9–O21	2.013(4)
Ca3–OW12	2.433(6)	<As3–O>	1.688	V3–O42	2.258(4)	V9–O39	2.278(4)
Ca3–OW3	2.435(5)			<V3–O>	1.946	<V9–O>	1.978
<Ca3–O>	2.389	As4–O12	1.664(3)				
		As4–O13	1.689(3)				
Ca4–O24	2.334(4)	As4–O14	1.694(4)	V4–O34	1.619(4)	V10–O51	1.593(4)
Ca4–O20	2.359(4)	As4–O15	1.695(4)	V4–O29	1.819(4)	V10–O40	1.783(3)
Ca4–OW15	2.382(5)	<As4–O>	1.686	V4–O19	1.982(4)	V10–O45	1.783(3)
Ca4–OW11	2.407(5)			V4–O38	2.003(3)	V10–O27	2.052(3)
Ca4–OW2	2.413(5)	As5–O16	1.661(4)	V4–O2	2.048(3)	V10–O6	2.078(3)
Ca4–OW29	2.534(6)	As5–O17	1.697(4)	V4–O43	2.238(3)	V10–O30	2.891(4)
Ca4–OW25	2.557(5)	As5–O18	1.699(3)	<V4–O>	1.952	<V10–O>	2.03
<Ca4–O>	2.427	As5–O19	1.707(4)				
		<As5–O>	1.691				
Ca5–OW27	2.360(5)			V5–O35	1.608(4)	V11–O47	1.600(4)
Ca5–O48	2.360(4)	As6–O20	1.663(4)	V5–O29	1.795(4)	V11–O41	1.776(3)
Ca5–OW18	2.410(5)	As6–O21	1.689(3)	V5–O23	1.967(4)	V11–O42	1.778(3)
Ca5–O32	2.470(4)	As6–O22	1.695(4)	V5–O39	1.998(3)	V11–O10	2.032(4)
Ca5–OW14	2.471(5)	As6–O23	1.701(4)	V5–O1	2.049(3)	V11–O13	2.081(3)
Ca5–OW4	2.510(4)	<As6–O>	1.687	V5–O44	2.270(4)	V11–O28	3.036(4)
Ca5–O31	2.523(4)			<V5–O>	1.948	<V11–O>	2.051
Ca5–O47	2.622(4)	As7–O24	1.651(3)				
<Ca5–O>	2.466	As7–O25	1.694(4)				
		As7–O26	1.702(4)	V6–O36	1.610(4)	V12–O49	1.588(4)
Ca6–OW37	2.341(9)	As7–O27	1.704(4)	V6–O30	1.804(4)	V12–O44	1.783(3)
Ca6–OW23	2.369(5)	<As7–O>	1.688	V6–O26	1.964(3)	V12–O43	1.796(3)
Ca6–OW21	2.406(7)			V6–O39	1.993(4)	V12–O18	2.024(4)
Ca6–OW36	2.437(7)			V6–O1	2.054(3)	V12–O22	2.048(4)
Ca6–O10	2.442(4)			V6–O45	2.292(4)	V12–O29	3.035(4)
Ca6–O13	2.491(4)			<V6–O>	1.953	<V12–O>	2.046
Ca6–OW35	2.578(8)						
Ca6–OW40	2.663(15)						
<Ca6–O>	2.466						

Bond valences are based upon Brown & Altermatt (1985) except those for Na^{+}–O which are based on Wood & Palenik (1999).

TABLE 7. CATION BOND VALENCE SUMS (BVS IN *vu*) AND V^{4+}/V^{5+} SITE OCCUPANCIES CALCULATED FROM BOND VALENCES IN VANARSITE*

Na, Ca, and As											
Atom	BVS	Atom	BVS	Atom	BVS	Atom	BVS	Atom	BVS	Atom	BVS
Ca1	1.99	Ca2	2.19	Ca3	2.24	Ca4	2.07	Ca5	2.13	Ca6	2.15
Na	1.04	As1	2.77	As2	4.97	As3	4.97	As4	4.99	As5	4.92
As6	4.97	As7	4.96								

V								
Atom	BVS	V^{4+}/V^{5+}	Atom	BVS	V^{4+}/V^{5+}	Atom	BVS	V^{4+}/V^{5+}
V1	4.52	0.48/0.52	V2	4.49	0.51/0.49	V3	4.64	0.36/0.64
V4	4.51	0.49/0.51	V5	4.67	0.33/0.67	V6	4.61	0.39/0.61
V7	4.13	0.87/0.13	V8	4.20	0.80/0.20	V9	4.18	0.82/0.18
V10	4.89	0.11/0.89	V11	4.90	0.10/0.90	V12	4.95	0.05/0.95

* Bond valences are based on Brown & Altermatt (1985) except those for Na^{+}–O that are based on Wood & Palenik (1999). Vanadium valences were calculated using program VaList (Wills 2011).

gatewayite did not allow the location of H atom sites. For the vanarsite structure, difference Fourier syntheses located all H atom positions (except those associated with four partially occupied H_2O groups) and the H positions were refined with soft restraints of 0.9(3) Å on the O–H distances and 1.42(3) Å on the H–H distances, and with the U_{eq} of each H set to 1.2× that of the donor O atom. All non-hydrogen atoms (except OW41 and OW42) were refined with anisotropic displacement parameters (on deposit).

Data collection and refinement details for all four structures are given in Table 4. Because of the very large number of independent atoms in each of these structures, complete structure details are reported here

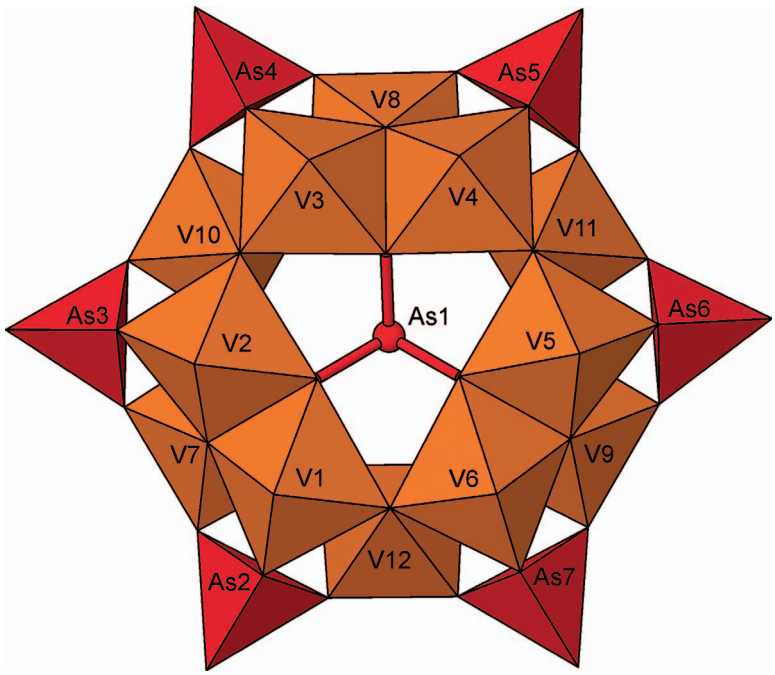

FIG. 10. The $[As^{3+}V^{4+,5+}{}_{12}As^{5+}{}_{6}O_{51}]$ heteropolyanion.

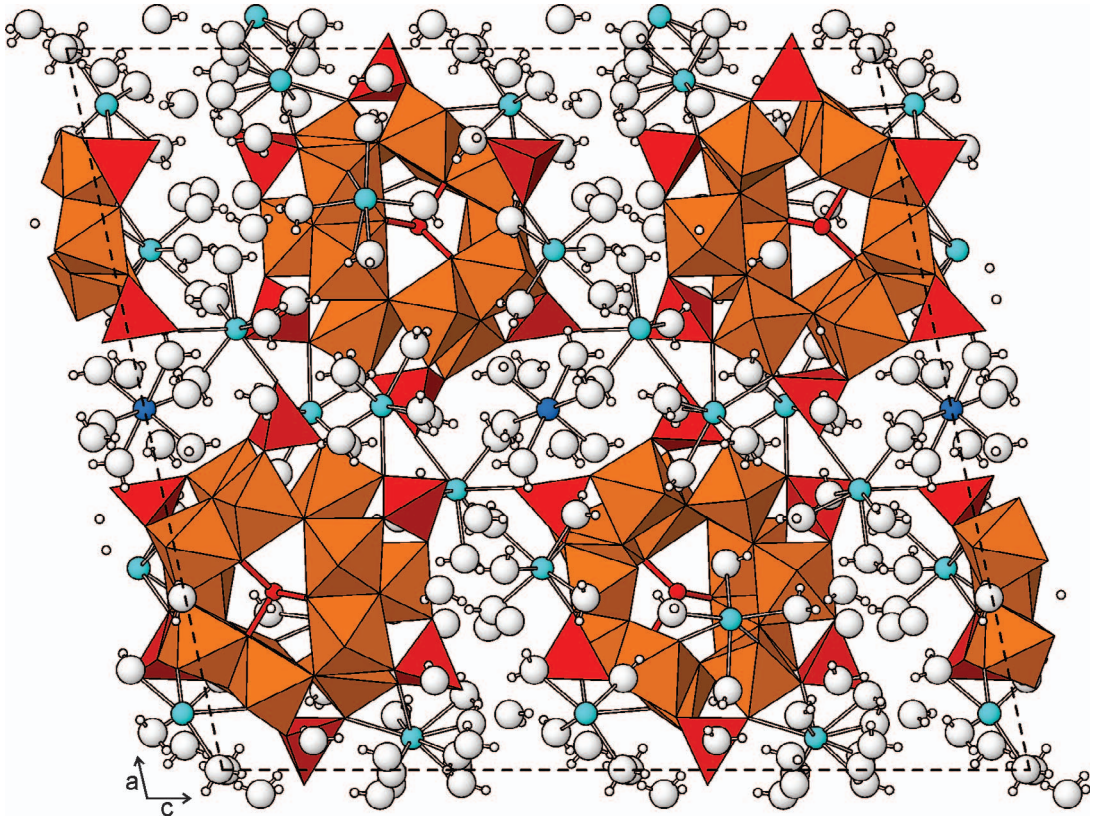

FIG. 11. Crystal structure of vanarsite viewed down [010]. Components of the anionic cluster are as labelled in Figure 10. Large white spheres are O atoms of H_2O groups. In this and subsequent figures, small white spheres are H atoms, light blue spheres are Ca atoms, and dark blue spheres are Na atoms. The unit cell outline is shown by a dashed black line.

only for vanarsite. The structure details for packratite, morrisonite, and gatewayite have been deposited. Atom coordinates and equivalent isotropic displacement parameters for vanarsite are reported in Table 5, selected bond distances in Table 6, and bond valences for all non-hydrogen cations and V^{4+}/V^{5+} occupancies in Table 7.

DESCRIPTIONS OF THE STRUCTURES

The structures of the vanarsite family minerals consist of two distinct parts, a structural unit and an interstitial unit, as suggested by Schindler & Hawthorne (2001) for such hydrated minerals with a polyanion. The structural unit in all four vanarsite-family minerals is a novel $[As^{3+}V^{4+,5+}{}_{12}As^{5+}{}_6O_{51}]$ heteropolyanion composed of twelve distorted $V^{4+,5+}O_6$ octahedra surrounding a central $As^{3+}O_3$ (arsenite) pyramid and decorated by peripheral $As^{5+}O_4$ (arsenate) tetrahedra, each of which shares three of its four vertices with VO_6 octahedra (Fig. 10). Bond valence calculations for the V sites (see Table 7 for vanarsite) indicate that they include a mixture of V^{4+} and V^{5+} and the dark blue color of the minerals results from V^{4+}–V^{5+} charge transfer. The stoichiometry and charge of the heteropolyanion varies from $[As^{3+}V^{4+}{}_2V^{5+}{}_{10}As^{5+}{}_6O_{51}]^{11-}$ to $[As^{3+}V^{4+}{}_{3.5}V^{5+}{}_{8.5}As^{5+}{}_6O_{51}]^{12.5-}$ (see Tables 1 and 2) and this serves to balance the charge of the interstitial unit, which differs in each of the four minerals.

In the structure of vanarsite (Fig. 11), the interstitial unit consists of seven isolated H_2O groups, one insular $Na(H_2O)_6$ octahedron, and six Ca–O polyhedra that are either seven- or eight-coordinated. The Ca–O polyhedra share two, three, or four of their vertices with O atoms of the VO_6 octahedra and/or AsO_4 tetrahedra of the structural unit. The remaining vertices of the Ca polyhedra are H_2O groups. The structural units are linked *via* the Ca–O polyhedra, as well as by an extensive system of hydrogen bonds. The

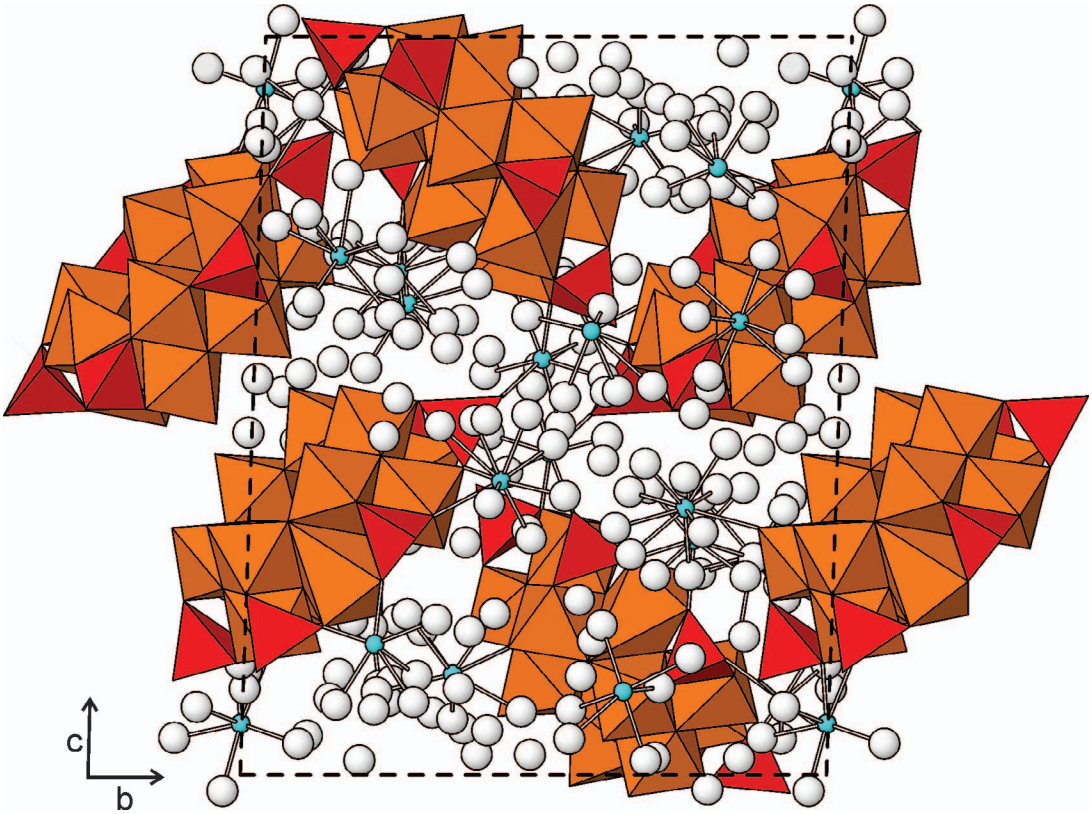

FIG. 12. Crystal structure of packratite viewed down [100]. Components of the structure are as labelled in Figures 10 and 11. The unit cell outline is shown by a dashed black line.

Ca2, Ca3, and Ca6 polyhedra each link to only one structural unit, whereas the Ca1, Ca4, and Ca5 polyhedra link to two adjacent structural units. Interestingly, none of the Na or Ca polyhedra link to one another. The interstitial unit, $[Na(H_2O)_6Ca_{12}(H_2O)_{58}{\cdot}14H_2O]^{25+}$, combines with two $[As^{3+}V^{5+}{}_{8.5}V^{4+}{}_{3.5}As^{5+}{}_6O_{51}]^{12.5-}$ polyanion structural units in the formula unit.

In the structure of packratite (Fig. 12), the interstitial unit consists of 24 isolated H_2O groups and eleven Ca–O polyhedra that are 7-, 8-, or 9-coordinated. The Ca–O polyhedra share one, two, or three of their vertices with O atoms of the VO_6 octahedra and/or AsO_4 tetrahedra of the structural unit. The remaining vertices of the Ca polyhedra are H_2O groups. The structural units are linked *via* the Ca–O polyhedra, as well as by an extensive system of hydrogen bonds. None of the Ca polyhedra links to another. The interstitial unit, $[Ca_{11}(H_2O)_{59}{\cdot}24H_2O]^{22+}$, combines with two $[As^{3+}V^{4+}{}_2V^{5+}{}_{10}As^{5+}{}_6O_{51}]^{11-}$ polyanion structural units in the formula unit.

Determining the final details of the atomic arrangement of morrisonite was somewhat problematic. In the structure of morrisonite (Fig. 13) the interstitial unit consists of 10 well-defined Ca–O polyhedra in all of which the Ca atom is seven-coordinated. These Ca–O polyhedra share one, two, or three of their vertices with O atoms of the VO_6 octahedra and/or AsO_4 tetrahedra of the structural unit. The remaining vertices of these Ca–O polyhedra are H_2O groups. The structural units are linked *via* the Ca–O polyhedra, as well as by an extensive system of hydrogen bonds. None of the well-defined Ca polyhedra links to another. Replicate chemical analyses of morrisonite demonstrated that an eleventh Ca atom exists within the interstitial unit. As no obvious Ca site was seen in difference maps, we must assume that the Ca atom is disordered among sites within the interstitial unit. For that reason, we examined all the sites that were modelled with oxygen scattering factors; it was found that the partially occupied sites O164, O171, O180, and O184, although refined with

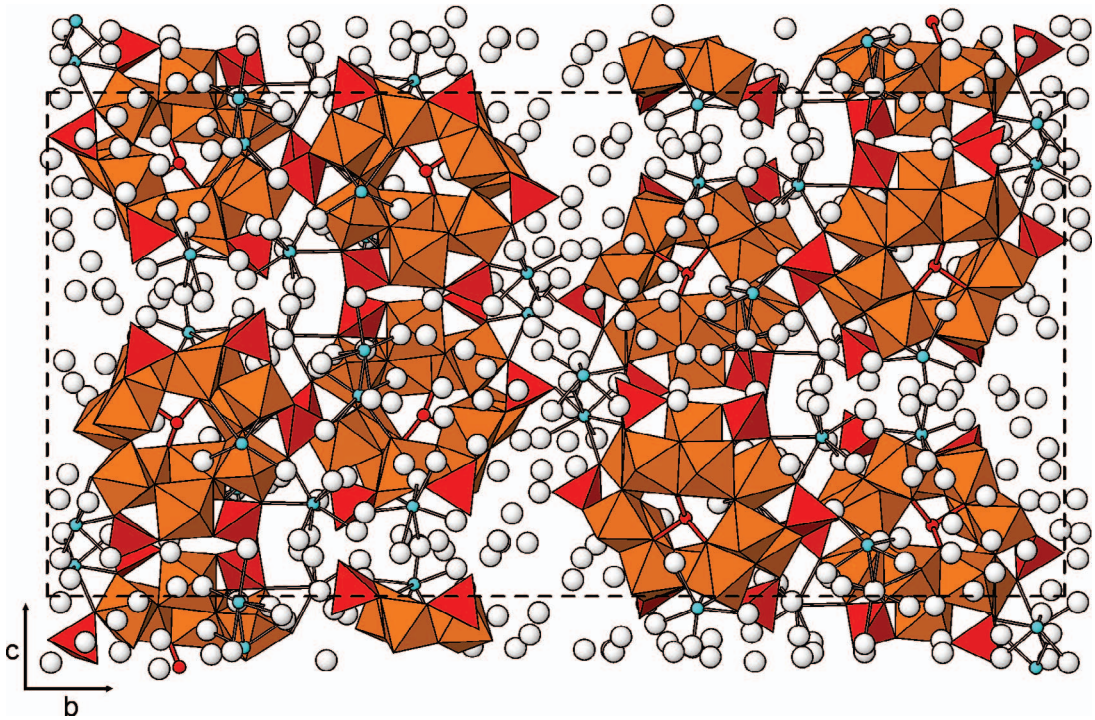

FIG. 13. Crystal structure of morrisonite viewed down [100]. Components of the structure are as labelled in Figures 10 and 11. The unit cell outline is shown by a dashed black line.

oxygen scattering factors, have bonding environments permissible for occupancy by Ca. It is also noteworthy that the displacement parameters of O164, O180, and O184 are non-positive definite. The structure refinement provides a total of about 182 O *apfu*; however, two of these must be deducted to allow for the eleventh Ca atom. Therefore, the formula basis is 180 O *apfu* with 102 O atoms in the structural unit and 78 in the interstitial unit. The interstitial unit, $[Ca_{11}(H_2O)_{78}]^{22+}$, combines with two $[As^{3+}V^{4+}{}_2V^{5+}{}_{10}As^{5+}{}_6O_{51}]^{11-}$ polyanion structural units in the formula unit. Better crystals will be required to unravel the final structural details of the morrisonite interstitial unit.

In the structure of gatewayite (Figs. 14 and 15), the interstitial unit consists of nine isolated H_2O groups, four of which are partially occupied, and six Ca–O polyhedra that are six- or seven-coordinated, although the coordination of the split Ca6 site is difficult to accurately define. The Ca–O polyhedra share one, two, or three of their vertices with O atoms of the VO_6 octahedra and/or AsO_4 tetrahedra of the structural unit. The remaining vertices of the Ca polyhedra are H_2O groups. The structural units are linked *via* the Ca–O polyhedra into a sheet parallel to {101} (Fig. 6). The Ca polyhedra do not link to one another. The only linkage between these sheets is *via* hydrogen bonds. The interstitial unit, $[Ca_6(H_2O)_{23}\cdot 8H_2O]^{12+}$, combines with the $[As^{3+}V^{4+}{}_3V^{5+}{}_9As^{5+}{}_6O_{51}]^{12-}$ polyanion structural unit in the formula unit.

Although the minerals of the vanarsite family contain a common structural unit in the $[As^{3+}As^{5+}{}_6V^{4+}{}_{2+x}V^{5+}{}_{10-x}O_{51}]^{(11+x)-}$ heteropolyanion, there appears to be no structural relationship among the lattice parameters of the vanarsite family minerals. In compounds such as these, wherein the structures are formed of rigid structural units that are linked by less-rigid interstitial units, similarities in lattice parameters are less common, particularly in compounds with different compositions of the interstitial unit, such as the vanarsite family.

POLYOXOMETALATES IN THE URAVAN ENVIRONMENT

Although As–V polyoxometalate compounds (arsenato-polyoxovanadates) have been extensively studied by inorganic chemists (*cf.* Wutkowski *et al.* 2011), synthetic studies have not yet yielded a cluster anion

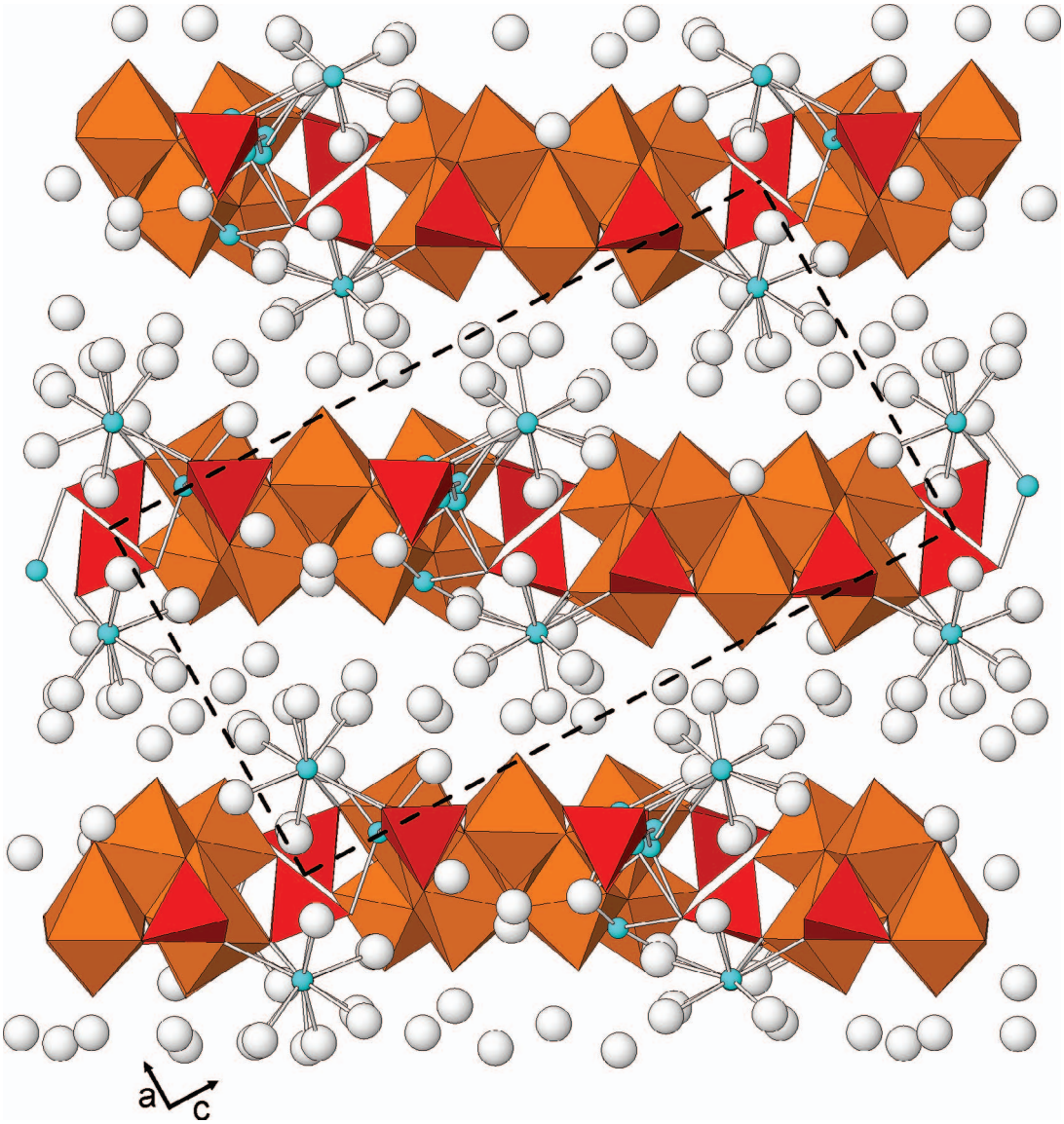

FIG. 14. Crystal structure of gatewayite viewed down [010]. Components of the structure are as labelled in Figures 10 and 11. The unit cell outline is shown by a dashed black line.

similar to that found in these minerals; indeed, the vanarsite family minerals are the only known minerals that contain both mixed-valence As and mixed-valence V.

The environment in which the vanarsite family minerals formed, in which natural phases form from the oxidation of montroseite–corvusite assemblages in a moist environment, has also yielded several variants of the decavanadate POM. Kampf *et al*. (2014a) summarized the recently discovered decavanadates from the area and showed that in addition to the previously described $[V^{5+}_{10}O_{28}]^{6-}$ decavanadates described from other environments, the Uravan region has yielded both protonated decavanadates, $[H_xV_{10}O_{28}]^{(6-x)-}$ and mixed-valence decavanadates, $[(V^{4+}_xV^{5+}_{10-x})O_{28}]^{(6+x)-}$, illustrating the complexity in that particular polyoxometalate that forms in nature.

Kampf *et al*. (2014b) recently described the mineral ophirite from the Ophir Hill Consolidated mine, Ophir District, Oquirrh Mountains, Tooele

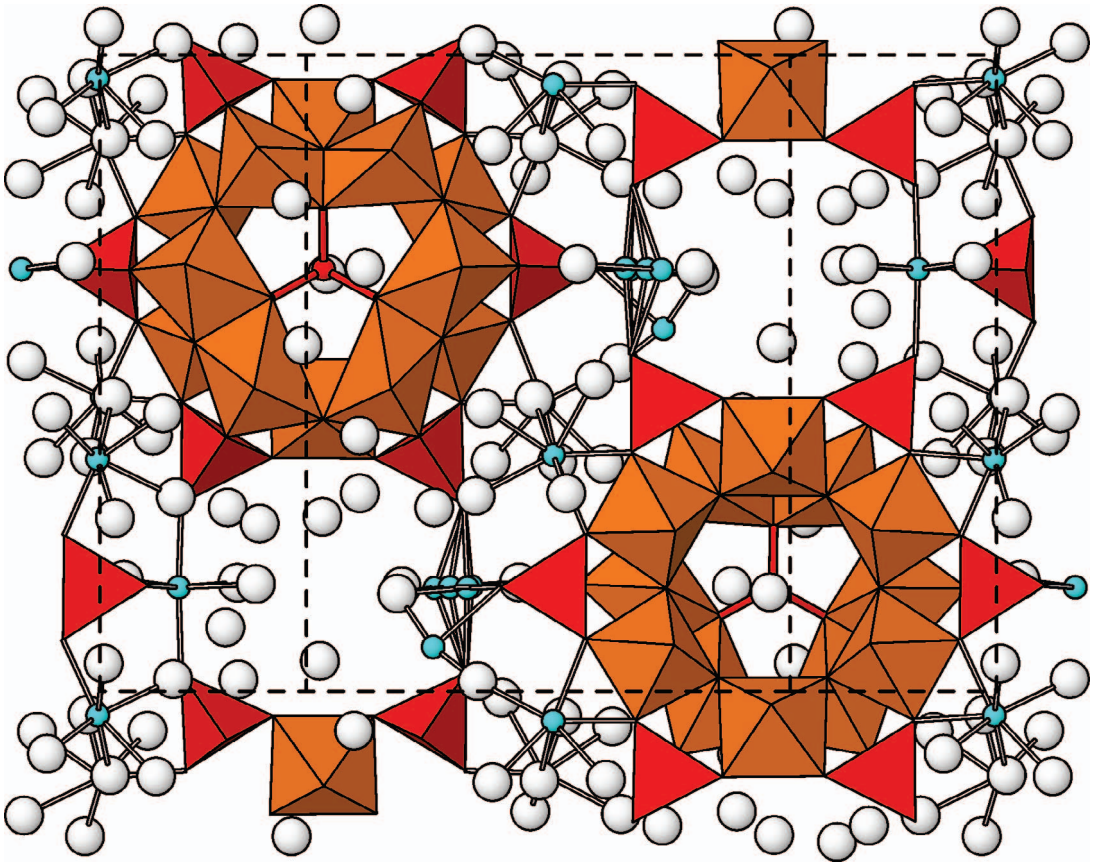

FIG. 15. Crystal structure of gatewayite viewed perpendicular to {101}. The *b* axis is vertical. The unit cell outline is shown by a dashed black line.

County, Utah, a different mineral environment from the conditions found in the Uravan belt. The structural unit of ophirite contains a heteropolytungstate tri-lacunary Keggin anion. The Keggin anion is formed of 12 M–O octahedra surrounding a central tetrahedral cation, X; the most common M cations are Mo and W. "Tri-lacunary" refers to the fact that three of the 12 M–O octahedra (all on the same side of the cluster) are missing. In ophirite, the Keggin anion is a tri-lacunary defect because of three missing octahedra. A comparison of the Keggin-anion portion of the ophirite structural unit, $(Fe^{3+}W_9O_{34})$ yields little similarity to the $[As^{3+}As^{5+}{}_6V^{4+}{}_{2+x}V^{5+}{}_{10-x}O_{51}]^{(11+x)-}$ structural unit in the vanarsite family. The only portion common to the Keggin polyanion and the vanarsite family polyanion is a puckered ring of six octahedra, but the octahedral trimers that are essential for the Keggin polyanion are not present in the $[As^{3+}V^{4+,5+}{}_{12}As^{5+}{}_6O_{51}]$ polyanion. There is no similarity other than they both are heteropolyanions.

ACKNOWLEDGMENTS

The authors are pleased to contribute this manuscript to a volume honoring our long-time colleague and friend Frank C. Hawthorne. There is no mineralogist who has contributed the volume, depth, and quality of insightful contributions to the broad discipline of mineralogy as has Professor Hawthorne, and we wish him well on the occasion of his 70th birthday and for continuing contributions to the discipline. We would like to thank Dick White, Race Fisher, Mike Palmer, at Energy Fuels Resources, and Jess W. Fulbright with San Juan Mine Rescue who made it possible for us to visit the Packrat Mine.

Reviewers R. James Evans, Paula C. Piilonen, and Henrik Friis are thanked for their constructive

comments on the manuscript. This study was funded, in part, by the John Jago Trelawney Endowment to the Mineral Sciences Department of the Natural History Museum of Los Angeles County and by grant NSF-MRI 1039436 from the National Science Foundation to JMH. The electron microprobe laboratory at the University of Utah is supported in part by the National Science Foundation, the College of Mines and Earth Sciences, and the Department of Geology and Geophysics. The assistance of Wil Mace with the EPMA is much appreciated.

References

Aureliano, M. (2011) Recent perspectives into biochemistry of decavanadate. *World Journal of Biological Chemistry* **2(10)**, 215–225.

Brown, I.D. & Altermatt, D. (1985) Bond-valence parameters from a systematic analysis of the inorganic crystal structure database. *Acta Crystallographica* **B41**, 244–247.

Burla, M.C., Caliandro, R., Camalli, M., Carrozzini, B., Cascarano, G.L., De Caro, L., Giacovazzo, C., Polidori, G., & Spagna, R. (2005) SIR2004: an improved tool for crystal structure determination and refinement. *Journal of Applied Crystallography* **38**, 381–388.

Carter, W.D. & Gualtieri, J.L. (1965) Geology and uranium–vanadium deposits of the La Sal quadrangle, San Juan County, Utah, and Montrose County, Colorado. *United States Geological Survey Professional Paper* **508**.

Cronin, L. & Müller, A. (2012) From serendipity to design of polyoxometalates at the nanoscale, aesthetic beauty and applications. *Chemical Society Reviews* **41**, 7333–7334.

Gunter, M.E., Bandli, B.R., Bloss, F.D., Evans, S.H., Su, S.-C., & Weaver, R. (2004) Results from a McCrone spindle stage short course, a new version of EXCALIBR, and how to build a spindle stage. *The Microscope* **52**, 23–39.

Higashi, T. (2001) *ABSCOR*. Rigaku Corporation, Tokyo, Japan.

Kampf, A.R., Hughes, J.M., Marty, J., Nash, B.P., Chen, Y.-S., & Steele, I.M. (2014a) Bluestreakite, $K_4Mg_2(V^{4+}{}_2V^{5+}{}_8O_{28})\cdot 14H_2O$, a new mixed-valence decavanadate mineral from the Blue Streak mine, Montrose County, Colorado: crystal structure and descriptive mineralogy. *Canadian Mineralogist* **52**, 1007–1018.

Kampf, A.R., Hughes, J.M., Nash, B.P., Wright, S.E., Rossman, G.R., & Marty, J. (2014b) Ophirite, $Ca_2Mg_4[Zn_2Mn^{3+}{}_2(H_2O)_2(Fe^{3+}W_9O_{34})_2]\bullet 46H_2O$, a new mineral with a heteropolytungstate tri-lacunary Keggin anion. *American Mineralogist* **99**, 1045–1051.

Pouchou, J.-L. & Pichoir, F. (1991) Quantitative analysis of homogeneous or stratified microvolumes applying the model "PAP." *In* Electron Probe Quantitation (K.F.J. Heinrich & D.E. Newbury, eds.). Plenum Press, New York, United States (3l–75).

Schindler, M. & Hawthorne, F.C. (2001) A bond-valence approach to the structure, chemistry, and paragenesis of hydroxyl-hydrated oxysalt minerals. I. Theory. *Canadian Mineralogist* **39**, 1225–1242.

Shawe, D.R. (2011) Uranium-vanadium deposits of the Slick Rock district, Colorado. *United States Geological Survey Professional Paper* **576-F**.

Sheldrick, G.M. (2008) A short history of SHELX. *Acta Crystallographica* **A64**, 112–122.

Song, Y.-F. & Tsunashima, R. (2012) Recent advances on polyoxometalate-based molecular and composite materials. *Chemical Society Reviews* **41**, 7384–7402.

Wills, A.S. (2011) VaList – Analysis of charge ordering and crystal structures using bond valence analysis. University College London, Department of Chemistry, London, England. <www.ucl.ac.uk/chemistry/staff/academic_pages/andrew_wills>. [date accessed: March 2015]

Wood, R.M. & Palenik, G.J. (1999) Bond valence sums in coordination chemistry. Sodium–oxygen complexes. *Inorganic Chemistry* **38(17)**, 3926–3930.

Wutkowski, A., Evers, N., & Bensch, W. (2011) Synthesis, structure, and solubility studies of a new arsenato-polyoxovanadate cluster compound: $(NH_4)_4[V_{12}As_8O_{40}(H_2O)]\cdot 4H_2O$. *Zeitschrift für anorganische und allgemeine Chemie* **637(14–15)**, 2205–2210.

Received May 22, 2015. Revised manuscript accepted October 2, 2015.